Title: HIGHLY MICROPOROUS CARBONS FROM OLIVE TREE PRUNING: OPTIMIZATION OF CHEMICAL ACTIVATION CONDITIONS

Authors: Mamaní Arminda, Sardella María Fabiana, Giménez Marianela, Deiana Cristina

PII: S2213-3437(18)30753-X
DOI: https://doi.org/10.1016/j.jece.2018.102830
Reference: JECE 102830

To appear in:

Received date: 24 August 2018
Revised date: 14 November 2018
Accepted date: 13 December 2018

Please cite this article as: Arminda M, Fabiana SM, Marianela G, Cristina D, HIGHLY MICROPOROUS CARBONS FROM OLIVE TREE PRUNING: OPTIMIZATION OF CHEMICAL ACTIVATION CONDITIONS, *Journal of Environmental Chemical Engineering* (2018), https://doi.org/10.1016/j.jece.2018.102830

HIGHLY MICROPOROUS CARBONS FROM OLIVE TREE PRUNING: OPTIMIZATION OF CHEMICAL ACTIVATION CONDITIONS

Mamaní Arminda*, Sardella María Fabiana, Giménez Marianela, Deiana Cristina

Instituto de Ingeniería Química, Universidad Nacional de San Juan-CONICET

San Juan Av. Libertador 1109(oeste), 5400 San Juan Argentina

armin7mamani@gmail.com

Graphical abstract

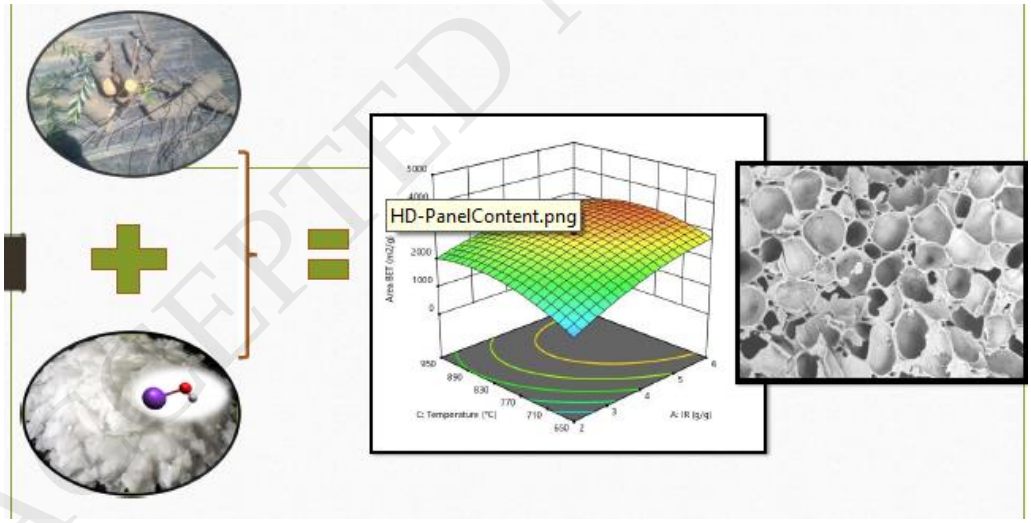

Highlights

- Olive tree pruning is a renewable and low-cost precursor for activated carbons.
- Highly microporous materials from olive tree pruning suitable for energy storage.
- Best activation conditions were determined through statistical optimization.
- Activation with KOH demonstrated to be efficient to obtain highly porous materials.

Abstract

The growing environmental problems and the depletion of fossil fuels have driven the research towards the development of renewable energy sources and the technologies that make use of them. In this context appears the demand of renewable, abundant and low-cost precursors as an alternative to traditional fossil sources. Activated carbons are materials with a great variety of applications which can be obtained from lignocellulosic wastes. This work evaluates the valorization of olive tree pruning (OTP) through the production of highly microporous carbons with KOH. A statistical optimization study was performed and the effect of the impregnation ratio, temperature and activation time on the developed surface area was studied. The optimum activation conditions for maximum porous development were: impregnation ratio of 6.38, 788.5°C and 145 minutes. Under these conditions 3514 m^2/g of surface area was generated, exceeding the values found in the bibliography. The sample obtained under optimal conditions was further characterized with SEM and FTIR and pH_{pzc}. From its characteristics it was concluded that activated carbons generated from olive tree pruning residues using KOH are suitable for applications such as adsorption, EDLC electrodes and gas storage, among others.

Keywords: olive tree pruning; activated carbons; valorization; central composite design; optimum conditions

1. Introduction

Environmental sustainability implies the constant search of processes that allow valorization of waste. Among them, agroindustrial wastes have gained special attention in the last years[1]. Lignocellulosic residues can be considered as potentially sustainable precursors in different fields[2, 3]. These residual biomasses can be subjected to thermal treatments to obtain different products of wide demand, such as activated carbons, which are materials with a highly developed internal porous structure, large surface area and high adsorptive capacity, which can be obtained from any carbon rich material[4, 5]. Important features of the raw materials chosen as precursors for activated carbon production are: low price, potential extent of its activation and also the stability of its supply[6]. The use of lignocellulosic residues as activated carbon precursors generally fulfills these conditions in addition to being renewable and relatively less expensive[7]. These porous materials are widely used for different applications such as: food purification, metal recovery, drinking water treatment, pollutant removal, among others[8]. The technological development expanded the applications of the activated carbons towards supercapacitors, electrodes and gas storage, which require a higher porous development and surface areas over 2000 m^2/g[9]. These materials are called super activated carbons and the study of the operating conditions necessary for their synthesis from low cost lignocellulosic materials has gain great attention in the last years [10-14].

Olive tree pruning (OTP) is the residue generated by the olive industry as a result of their agricultural labors. Nowadays, about 11 million hectares are used for olive trees cultivation all around the world, with an annual production of pruning residue estimated at 3000 kg/ha[15]. Due to its low humidity content the degradation by aging is extremely low and the removal of this residual biomass is imperative to keep fields clean and to avoid plant diseases propagation. This residual material has good properties to produce activated carbons, one of the most used adsorbents and other applications, generating economic benefits that can eventually offset the costs of treatment and disposal. So, considering OTP as a byproduct of this agroindustrial activity, useful as porous materials precursor, has environmental and economic benefits [2, 16-18].

There are two methods to obtain activated carbon, physical and chemical activation [19-21]. In chemical activation, the precursor is impregnated with a chemical activating agent such as $ZnCl_2$, H_3PO_4, KOH, H_2SO_4 and NaOH, followed by carbonization[22, 23]. Among chemical activating agents, KOH is generally preferred since it is less aggressive to the environment than other agents, such as H_3PO_4 and $ZnCl_2$, leads to higher surface area development and yields porous materials with an improved electrochemical performance[24, 25]. Another advantage of using KOH is that the K_2CO_3 formed after the interaction between KOH and carbon can prevent from excessive combustion of the sample, resulting in high performance and well-developed internal porosity[26].

According to previous studies[27] the activation process with KOH takes place in three steps. In the first step, potassium reacts with the carbonaceous components of the charcoal and form the carbon structure with the porous

network architecture. In the second stage, the steam and carbon dioxide produced react with the carbonaceous material at high temperatures, which is actually a physical activation process that contributes to carbon porosity development. The third step involves the diffusion of the formed metallic potassium towards the carbon matrix resulting in carbon lattices[28]. The specific activation processes are as follows:

$$6\,KOH + 2C \rightarrow 2K + 3H_2 + 2K_2CO_3$$

$$K_2CO_3 \rightarrow K_2O + CO_2$$

$$CO_2 + C \rightarrow 2CO$$

$$K_2CO_3 + 2C \rightarrow 2K + 3CO$$

$$K_2O + C \rightarrow 2K + CO$$

The interval in which all the reactions take place goes from 530°C to 827°C[27, 29]. The degree of advancement of the mentioned steps depends on the activation temperature selected. However, the reactivity of different raw precursors at various experimental conditions is difficult to predict. For this reason, it is important to analyze different activation conditions for the lignocellulosic waste studied in this work.

The preparation of carbons activated using KOH is influenced by many factors. Those reported in the literature as most influential are: impregnation ratio, temperature and activation time [30-32]. The use of an adequate experimental design is important to optimize the preparation conditions[33]. A conventional technique for the optimization of a multi-factorial system is to deal with one variable at a time (OFAT), a time consuming method which does not reveal the

interactive effects and that can miss optimal settings of factors. Response surface methodology (RSM), a method based on statistical principles, improves the prediction of the response in the factor space by reducing the variability of the estimates, and gives the optimal solution over the entire factor space. RSM is employed in this work as a strategy to study individual as well as interactive effects of the activating process parameters over activated carbons porosity. Significant information regarding the optimum set of levels of the activation process was also generated[34].

The aim of this work is to carry out a statistical optimization to determine the optimum preparation conditions of activated carbons with KOH from OTP using RSM based on central composite design (CCD). The effect of temperature, time and chemical impregnation ratio (KOH:charcoal) over the textural properties of the porous materials of the product were studied simultaneously. The activated carbons produced under the optimal conditions and any samples of design were characterized by their main textural properties.

2. Materials and methods

2.1 OTP characterization

For the development of this study, residues of olive tree pruning (*Olea europaea*), Manzanilla variety, was used. This material, called OTP, was submitted to size reduction, sieved and dried at room temperature. Proximate analysis was performed following ASTM D 4442-92, ASTM D 1102-84 and ASTM E 872-82 standards for moisture, ash and volatile matter content respectively. Fix carbon content was obtained by difference. Ultimate analysis was made in a Perkin Elmer 2400 Series II elemental analyzer.

The lignocellulosic composition of the materials was determined through neutral detergent fiber (NDF) and acid detergent fiber (ADF) content, determined on an automatic ANKOM A2000, following TAPPI T22 method. The difference between these values established the proportion of hemicellulose, while cellulose concentration was obtained by difference between acid detergent fiber and lignin content. The thermogravimetric (TG) and derivative thermogravimetric (DTG) analyses were carried out on a SHIMADZU DTG-60/60H thermal analysis instrument at a heating rate of 10°C.min^{-1} in N_2 atmosphere.

2.2 Carbonization

For activated carbons preparation the fraction of OTP particles with sizes comprised between 10-15 mm were used. This material was carbonized in an electrically heated stainless-steel reactor in the absence of oxygen. The heating rate was 4°C.min-1, from room temperature to a final temperature of 500 ° C, which was kept constant for 2 hours. Then the carbonized material was taken to a granulometry comprised between 5 and 1mm.

2.3 Activation with KOH

The charcoal produced was mixed with KOH solutions using different impregnation ratios (IR), which refers to the mass of impregnant with respect to the mass of the charcoal (equation 1). The mixture was then dehydrated in oven overnight at 130°C. The activation was carried out in a muffle furnace at different conditions, determined by the experimental design, which are shown in Table 2. The discharge product was cooled to room temperature, neutralized with a 0.5M HCl solution and washed with distilled water until a pH value between 6 and 7. Then it was filtered and finally dried at 130°C.

Equation 1 $$IR = \frac{mass\ of\ KOH(g)}{mass\ of\ carbonized\ OTP(g)}$$

2.4 Experimental design for activated carbon preparation

A standard design, called central composite design (CCD), was applied in this work to study the influence of certain preparation variables over the obtained activated carbons properties. The variables studied were activating agent:charcoal ratio, called impregnation ratio (IR) and labeled A, activation time (B) and temperature (C). The BET surface area, expressed in $m^2 . g^{-1}$, was chosen as response variable (Y) to evaluate the effect of these three variables together. Table 1 show the lower and upper limits chosen for each variable, based on literature and preliminary studies[30, 35]. A total of 17 experimental runs were necessary to perform the central composite design (CCD). The order of the experiments was completely randomized in order to minimize effects of the uncontrollable factors. The response variable (A_{BET}) was used to develop an empirical model.

Optimization of variables using experimental design was performed finding the stationary point of the model adjusted:

Equation 2 $$\hat{Y} = \hat{\beta} + \sum_{i=1}^{k} \hat{\beta}_i x_i + \sum_{i=1}^{k} \hat{\beta}_{ii} x_{ii}^{2} + \sum_{i=1}^{k} \sum_{<j=1}^{k} \hat{\beta}_{ij} x_i x_j$$

Which can be written in matrix form as follows:

Equation 3 $$\hat{Y} = \hat{\beta}_0 + x' b + x' B_x$$

Where x' = (x_1, x_2,…, x_k) is any point within the operating region, vector b contains all the coefficients of the linear part of the model (principal effects) matrix B contains the coefficients of interaction and purely quadratic terms

The optimization problem for this case can be formulated as:

$$\text{Max } Y(x_1, x_2, \ldots, x_k)$$

And optimal conditions can be found as follows:

$$\text{Equation 4} \qquad \frac{\partial \hat{Y}}{\partial x} = b + 2Bx = 0$$

Commercial software (Design expert 11.0.3 Inc.) was used to analyze the experimental results and find the optimal operating conditions. Table 2 shows the experimental design matrix.

2.5 Response variable determination

Nitrogen adsorption isotherms at 77K were determined using an ASAP 2000 - Micromeritics. Before the adsorption analysis the samples were outgassed at 250°C for 12 h. The total pore and micropore volumes were obtained by the application of Gurvich's rule at P/P_0 0.98 and Dubinin Radushkevich (w_0) model, respectively. Surface areas were determined using BET model.

Unlike other authors [36, 37] who calculate the yield as the ratio of activated carbon and carbonized material, in this case a global yield, which includes the carbonization and activation stages, is obtained. The yield of every experimental run, represented by the ratio of final weight of product to the initial weight of precursor, was calculated based on the following equation:

Equation 5 $$Y(\%) = \frac{weight\ of\ activated\ carbon}{weight\ of\ OTP} \times 100$$

2.6 Validation and characterization of optimum

The validation step consisted in contrasting the experimental results against the values predicted by the model obtained in the experimental design analysis. Experimental assays under the optimum conditions were performed by triplicate and named Q_{OP}. Optimum conditions were 788.5°C, IR of 6.38 and 145.25 minutes of activation.

Fourier Transform Infrared (FTIR) Spectroscopy (Paragon 1000PC -Perkin Elmer) was used to qualitatively determine the available effective groups on Q_{OP} surface. Scanning electron microscopy (SEM) JEOL JSM-6610LV was applied to study the morphology and porosity of the activated carbon prepared under the optimum conditions.

The point of zero charge was estimated from the pH of a concentrated dispersion following the method proposed by Noh and Schwarz[38]. Three aqueous solutions of different initial pH were prepared from a 0.01 M $NaNO_3$, using 0.01 M NaOH and 0.01 M HNO_3 for its regulation. The adsorbent was contacted with these solutions under different mass/volume ratios. The suspensions were placed in a shaker at room temperature for 4 days and the equilibrium pH was measured (HANNA HI1296).

3. Results and discussion

3.1 OTP and activated carbons characterization

The results of OTP characterization can be seen in Table 3, where it is possible to observe that this residue shows a proximate analysis typical of biomass[39,

40]. OTP has high carbon with low ash content indicated that the precursor is suitable activated carbon production[1]. In addition, it is important to highlight the low content in sulphur and nitrogen, which is advantageous for environmental reasons[41]. Content of lignin and cellulose affect the porous structure of the activated carbon[42, 43], the large percentage of cellulose compared to lignin could generated microporous carbons from this agricultural residue. Figure 1 presents the thermal decomposition behavior of OTP in a N_2 flow (100 ml.min^{-1}). The precursor weight loss as a function of pyrolysis temperature is measured from the thermogravimetric curves and shows that the pyrolysis behavior of OTP is similar to that of other lignocellulosic biomasses. It can be seen that the weight loss mainly occurred between 200°C and 600°C, with three stages. The first stage (temperature below 200°C) corresponds to the drying period, where water is liberated from the material. The second step involves the material devolatilization and it is the major step in all thermochemical conversion process involving biomass. It takes place at temperatures between 200 to 500^0 C, where a remarkable slope of the TG curve is observed, corresponding to the liberation of volatile hydrocarbon from the decomposition of hemicellulose, cellulose and some part of lignin. For stage 3, weight loss is not as significant as in stage 2, and it is attributed to the steady decomposition of the remaining heavy components mainly from lignin. In general, the weight losses of OTP at the range of 200–600°C are larger than those over 600°C because the lignin is more inclined to form char than hemicellulose and cellulose.

Figure 1

The specific surface areas, pore volumes and carbon yields of activated carbons can be seen in table 4. As it can see the values of surface areas vary according to activation conditions, the values range from 800 m^2/g (0.65 g of KOH/g carbonized OTP, 800°C and 82.5 minutes) to 3490 m^2/g (7.35 g of KOH/g carbonized OTP, 800°C and 82.5 minutes), while the total pore volume ranges from 0.33 cm^3/g to 1.66 cm^3/g respectively. These properties depend strictly on the time, the temperature and the impregnation ratio, it could be said that there is a direct relationship between IR and surface area, by increasing the ratio of KOH/charcoal there is more porous development. For temperature and IR, it is not so easy to make a relationship, since the reactions that develop porosity in the material depend on the temperature. When the temperature exceeds 950°C, micropores rupture seems to occur, and at low temperatures the reactions necessary to generate vacancies in the precursor are not completed[44].

Most of the activated carbons present high percentage of micropore volume (see Table 4). The yields also vary according to the conditions. The highest activation yield reached was 24.03%, obtained under conditions of Q_3 assay, and the lowest one (10.67%) was obtained under Q_9 conditions. These variations may be associated with mild and severe conditions applied in each experiment [35, 45-47]. It is noteworthy the highest porous development is not associated with lower yields, specific surface areas around 3000 m^2/g (samples Q_2 and Q_8) presented yields close to 20%. This is attributed to the activation mechanism, which involves chemical and physical activation, and makes the relation between surface area and yield not direct [27].

As the mechanism is not simple and involves different mechanisms (chemical and physical activation) the relation between variables and results is not easy. This means, as mentioned in the manuscript, there is not a direct relation between surface area and yield.

These results indicate that the OTP is appropriate for preparing ACs with large specific surface areas and very high micropore volumes, working under the adequate experimental conditions. Therefore, this material can be used in special applications that require elevated specific surfaces, such as supercapacitors, electrodes and gas storage[4, 9].

3.2 Statistical analysis of the results

Application of CCD for activated carbons production generated the following second order polynomial equation for the specific surface area:

$$A_{BET} = -1680 + 1400 \times A - 3.5 \times B + 40 \times C + 0.60 \times A \times B - 0.74 \times A \times C - 70 \times A^2 + 0.03 \times B^2 - 0.02 \times C^2 \qquad \text{Equation 4}$$

The model was evaluated by its correlation coefficient R^2, that was found to be 90.26%, and R^2adjusted=77.27%. These values are high enough to state the model fitted well the experimental data. The R^2-value implies that 90.26% of the response variable variation is attributed to the factors influence, so 9.74% of the total variation is not explained by the model and are not predictable results.

The results of the ANOVA are shown in Table 5. The purpose of this analysis is to investigate which operation variable significantly affects the development of porosity. In this case A (impregnation ratio) and C^2 (temperature) have significant influence on surface area of ACs, with p-value lower than the level of significance α = 0.05. In addition, the analysis shows that the model obtained to

represent the process has an F-value of 5.16, which implies the model is significant. The possibility of obtaining an F-value this large due to noise has a chance of only 4.28%.

From the model it was possible to calculate the optimal values of the factors to maximize the surface area, which are shown in table 3. The surface area predicted by the model was 3536.14 m^2/g. Assays under the optimum conditions were carried out by triplicate and an average surface area of 3514.25 m^2/g was obtained, a value only 0.6% below the one predicted, showing the reliability of the model obtained. The characteristics of Q_{op} were 1.79 and 1.20 $cm^3.g^{-1}$ pore volume and micropore volume respectively, with a yield of 15.53%. Its percentage of micropores was 67.43%.

The significant interactions of impregnation ratio, time and temperature response surfaces for BET area are presented in figures 2a, 2b and 2c. The surface generated from temperature and impregnation ratio interaction is concave, which allows finding the inflection and therefore the optimal conditions. To have a better illustration of the effects of factors over the activation process, the contour diagram of the most influential factors (temperature and IR) is presented in figure 3. It can be noticed that the optimum conditions found are within the region of the highest surface areas.

Figures 2a, 2b, 2c

Figure 3

3.3 Optimum characterization

3.1.1 Textural properties

Figure 4 shows the N_2 adsorption-desorption isotherms for Q_2, Q_{13}, Q_{15} and Q_{OP} samples. All isotherms are type I, according to the IUPAC classification, characteristic of microporous materials. Similar results have been reported for the activated carbons made from other precursors[48]. Isotherms of samples Q_{15}, Q_{13} and Q_{OP} present a small hysteresis loop, indicating the existence of mesopores. Anyway, the horizontal plateau observed in the middle range of P/Po suggest the preponderance of micropores over mesopores.

Figure 4

Micropores can be divided into ultramicropores (pores smaller than 0.7 nm) and supermicropores (pores sizes between 0.7–2 nm)[49, 50]. Figure 5 presents the pore size distribution (PSD) obtained for Qop sample. The existence of supermicropores makes this activated carbon suitable for its application in incoming technologies, such as such as double-layer electric capacitors, also known as supercapacitors[51].

Figure 5

Table 6 shows the results of carbons obtained from different lignocellulosic residues activated with KOH by other authors. It can be seen that olive tree pruning activated carbon obtained under optimum conditions offers the highest surface area value. This result makes this material attractive for special applications which require high microporosity, as energy storage.

3.3.2 Surface chemistry

The chemical structure of OTP, carbonized OTP and activated carbon prepared under optimum conditions QOP was analyzed by IR spectroscopy. Figure 6 and

table 8 provide information of the chemical structure and the changes in the functional groups.

Figure 6

The wide band observed around 3400 cm^{-1} represented the O–H stretching vibration in aromatic and aliphatic structure, the absorption observed at around 2920 cm^{-1} can be attributed to the stretching vibration of the C–H group. A band at 1720 cm^{-1}, indicative of C=O stretching vibration of nonaromatic carboxyl groups, appears with higher intensity in the OTP spectrum. The bands at 1626, 1522, and 1427 cm^{-1} were attributed to aromatic skeleton vibrations, whereas the band at 1427cm^{-1} corresponded to the C–H asymmetric vibrations and deformation was also observed. Band at 1250 cm^{-1} can be ascribed to C-O stretching. FTIR analysis it can be said there is presence of surface functional groups containing oxygen on the Q_{OP} surface[57].

The point of zero charge is defined as the pH value at which the total surface charge is zero and it was determined through the mass titration method[65]. Figure 7 shows the variation in pH as a function of the mass of activated carbon used in the suspension.

Figure 7

From this graphic, point zero charge of Qop was determined, showing it has basic properties with pH_{pzc} of 8.62. It is well documented that high contents of carbonyl, pyrone, and chromenes give basic character to the materials[66]. Therefore, the basic character of Q_{OP} could be attributed to the presence of these groups, which agrees with the FTIR analysis results. The basic character of this activated carbon can be advantageous for several reasons. It is known that adsorption capacity often decreases after long storage periods in the presence of

moisture[67]. Carbons with basic properties are much more resistant to this effect[68]. It has also been reported that the affinity of phenolic compounds increase with the basicity (hydrophobicity) of the carbon surface [69, 70]. The adsorption capacity of SO_2 in activated carbon increases with basic surface groups [71]. On the other hand, these groups can contribute to the capacity of the material due to pseudo capacity phenomena, improve wettability, facilitate electronic transfer processes and increase the stability of the carbonaceous material[72]. This last advantage is important if activated carbons are evaluated as supercapacitors.

3.3.3 M*orphological properties*

The micrographs of OTP, Q_2, Q_{13}, Q_{15} and Q_{OP} are shown in Figure 8. Precursor micrograph, figure 8a, showed a smooth surface with the longitudinal fibers of wood clearly marked[73]. Figures 8b, 8c, 8d and 8e of Q_2, Q_{13}, Q_{15} and Q_{OP} respectively show irregular cavities that have cracks and small holes. Q_2 and Q_{13} present heterogeneous structures, with irregularities and holes of various sizes, very different to the one observed in the raw material (figure 8a). The change on the surface topology is notable for Q_2, possibly associated to a higher RI applied. Images of Q_{15} and Q_{OP} show the generation of cavities uniformly distributed, which is almost perfect for Q_{OP}. All activated carbons kept the morphological structure of the precursor [74]. The differences observed on the activated carbons surfaces obtained under different conditions, showed the effect of the impregnation ratio, that is the interaction between carbon and KOH[35]. This proves that activating under optimum conditions causes the best and uniform porous development. As it could be verified in this work the thermal

treatment and the ratios of agent activating/charcoal suitable are extremely crucial to develop porosity.

Figure 8a

Figure 8b

Figure 8c

Figure 8d

Figure 8e

Conclusions

A statistical optimization of olive tree pruning residues (OTP) activation, with KOH as activating agent, was performed using a central composite design. The influence of the impregnation ratio (KOH:charcoal), activation temperature and activation time over the surface area (BET area) was studied. The high specific surface areas obtained, indicating the suitability of olive tree pruning as precursor for the preparation of highly microporous carbons.

An empirical model that correlated the specific surface area with the three variables studied was developed. From this equation the optimum conditions were obtained: KOH/carbon impregnation ratio: 6.38, temperature 788.5 °C and time 145 minutes. Validation of the model was carried out and difference between the predicted value and the real one was below 1%. Under the optimal operation conditions a highly porous carbon, with a surface area of 3514 m^2/g, was obtained.

The N_2 adsorption isotherm of the activated carbon obtained under optimum conditions (Q_{OP}) was Type I with a small hysteresis loop, indicating the existence of micropores and mesopores. The pore size distribution confirmed this characteristic and showed that the micropores are mostly supermicropores. The point of zero charge (pH_{pzc}) and FTIR analysis of Qop evidenced the basic character of the material. All these characteristics make this material very adequate for applications such as adsorbents, EDLC electrodes, dye adsorption, volatile organic compounds removal among others.

These results show that olive tree pruning residue constitutes a sustainable source for energy storage and novel materials production. The study of the best paths to achieve these objectives should continue.

Acknowledgements

This work was partially funded by following Argentine institutions: National Council of Scientific and Technical Research (CONICET), Universidad Nacional de San Juan.

References

1. Ioannidou, O. and A. Zabaniotou, *Agricultural residues as precursors for activated carbon production—A review.* Renewable and Sustainable Energy Reviews, 2007. **11**(9): p. 1966-2005.
2. M.I. Norlia, C.A.R., T.I.T. Nuraiti, M.Z.M. Salwa, M.S.S. Fatimah, *Preparation and Characterisation of Activated Carbon from Rambutan Seed (Nephelium Lappaceum) by Chemical Activation.* Empowering Science, Technology and Innovation Towards a Better Tomorrow, 2006.
3. Khadija Qureshi, I.B., Rafique Kazi , Abdul Khalique Ansari, *Physical and Chemical Analysis of Activated Carbon Prepared from Sugarcane Bagasse and Use for Sugar*

Decolorisation. International Journal of Chemical and Biomolecular Engineering, 2008. **3**: p. 145-149.

4. González-García, P., *Activated carbon from lignocellulosics precursors: A review of the synthesis methods, characterization techniques and applications.* Renewable and Sustainable Energy Reviews, 2018. **82**: p. 1393-1414.
5. Mohamad Nor, N., et al., *Synthesis of activated carbon from lignocellulosic biomass and its applications in air pollution control—a review.* Journal of Environmental Chemical Engineering, 2013. **1**(4): p. 658-666.
6. Ali, I., M. Asim, and T.A. Khan, *Low cost adsorbents for the removal of organic pollutants from wastewater.* J Environ Manage, 2012. **113**: p. 170-83.
7. Foo, K.Y. and B.H. Hameed, *Utilization of biodiesel waste as a renewable resource for activated carbon: Application to environmental problems.* Renewable and Sustainable Energy Reviews, 2009. **13**(9): p. 2495-2504.
8. Yahya, M.A., Z. Al-Qodah, and C.W.Z. Ngah, *Agricultural bio-waste materials as potential sustainable precursors used for activated carbon production: A review.* Renewable and Sustainable Energy Reviews, 2015. **46**: p. 218-235.
9. Abioye, A.M. and F.N. Ani, *Recent development in the production of activated carbon electrodes from agricultural waste biomass for supercapacitors: A review.* Renewable and Sustainable Energy Reviews, 2015. **52**: p. 1282-1293.
10. Yang, R., et al., *Preparation and N2, CO2 and H2 adsorption of super activated carbon derived from biomass source hemp (Cannabis sativa L.) stem.* Microporous and Mesoporous Materials, 2012. **158**: p. 108-116.
11. Nowicki, P., H. Wachowska, and R. Pietrzak, *Active carbons prepared by chemical activation of plum stones and their application in removal of NO2.* J Hazard Mater, 2010. **181**(1-3): p. 1088-94.
12. Gueye, M., et al., *High efficiency activated carbons from African biomass residues for the removal of chromium(VI) from wastewater.* Journal of Environmental Chemical Engineering, 2014. **2**(1): p. 273-281.
13. Rosas, J.M., et al., *Kinetic study of the oxidation resistance of phosphorus-containing activated carbons.* Carbon, 2012. **50**(4): p. 1523-1537.
14. Sun, K. and J.c. Jiang, *Preparation and characterization of activated carbon from rubber-seed shell by physical activation with steam.* Biomass and Bioenergy, 2010. **34**(4): p. 539-544.
15. Encarnación Ruiz, C.C., Mercedes Ballesteros, Paloma Manzanares, Ignacio Ballesteros, and Eulogio Castro, *Ethanol Production From Pretreated Olive Tree Wood and Sunflower Stalks by an SSF Process.* Applied Biochemistry and Biotechnology, 2007. **129-132**.
16. Williams, P. and A. Reed, *Development of activated carbon pore structure via physical and chemical activation of biomass fibre waste.* Biomass and Bioenergy, 2006. **30**(2): p. 144-152.
17. Adegoke, K.A. and O.S. Bello, *Dye sequestration using agricultural wastes as adsorbents.* Water Resources and Industry, 2015. **12**: p. 8-24.
18. Samorn Hirunpraditkoon, N.T., Anotai Ruangchai, and Kamchai Nuithitikul, *Adsorption Capacities of Activated Carbons Prepared from Bamboo by KOH Activation.* Chemical and Molecular Engineering, 2011. **5**.
19. Jun'ichi Hayashi , T.H., Isao Takeda, Katsuhiko Muroyama, Farid Nasir Ani, *Preparing activated carbon from various nutshells by chemical activation with K_2CO_3.* Carbon, 2002. **40**: p. 2381-2386.
20. Suhas, P.J. Carrott, and M.M. Ribeiro Carrott, *Lignin--from natural adsorbent to activated carbon: a review.* Bioresour Technol, 2007. **98**(12): p. 2301-12.
21. Ali, I., *The Quest for Active Carbon Adsorbent Substitutes: Inexpensive Adsorbents for Toxic Metal Ions Removal from Wastewater.* Separation & Purification Reviews, 2010. **39**(3-4): p. 95-171.

22. Kılıç, M., E. Apaydın-Varol, and A.E. Pütün, *Preparation and surface characterization of activated carbons from Euphorbia rigida by chemical activation with ZnCl2, K2CO3, NaOH and H3PO4.* Applied Surface Science, 2012. **261**: p. 247-254.
23. Demiral, H., et al., *Pore structure of activated carbon prepared from hazelnut bagasse by chemical activation.* Surface and Interface Analysis, 2008. **40**(3-4): p. 616-619.
24. Donald, J., Y. Ohtsuka, and C. Xu, *Effects of activation agents and intrinsic minerals on pore development in activated carbons derived from a Canadian peat.* Materials Letters, 2011. **65**(4): p. 744-747.
25. Deng, H., et al., *Preparation of activated carbons from cotton stalk by microwave assisted KOH and K2CO3 activation.* Chemical Engineering Journal, 2010. **163**(3): p. 373-381.
26. Hui, T.S. and M.A.A. Zaini, *Potassium hydroxide activation of activated carbon: a commentary.* Carbon letters, 2015. **16**(4): p. 275-280.
27. Gao, Z., et al., *Biomass-derived renewable carbon materials for electrochemical energy storage.* Materials Research Letters, 2016. **5**(2): p. 69-88.
28. Ahmed, M.J. and S.K. Theydan, *Adsorption of cephalexin onto activated carbons from Albizia lebbeck seed pods by microwave-induced KOH and K2CO3 activations.* Chemical Engineering Journal, 2012. **211-212**: p. 200-207.
29. Huang, Y., E. Ma, and G. Zhao, *Thermal and structure analysis on reaction mechanisms during the preparation of activated carbon fibers by KOH activation from liquefied wood-based fibers.* Industrial Crops and Products, 2015. **69**: p. 447-455.
30. Salman, J.M., *Optimization Study of Pesticides Removal by Olives Trees Stalks Activated Carbon Using Response Surface Methodology.* 2015.
31. Abdel-Ghani, N.T., et al., *Optimizing the preparation conditions of activated carbons from olive cake using KOH activation.* New Carbon Materials, 2016. **31**(5): p. 492-500.
32. Niasar, H.S., et al., *Preparation of activated petroleum coke for removal of naphthenic acids model compounds: Box-Behnken design optimization of KOH activation process.* J Environ Manage, 2018. **211**: p. 63-72.
33. Calado, D.G.a.V.M.d.A., *The use and importance of design of experiments (DOE) in process modelling in food science and technology*. Mathematical and Statistical Methods in Food Science and Technology,. Vol. 1. 2014.
34. Salman, J.M., *Optimization of preparation conditions for activated carbon from palm oil fronds using response surface methodology on removal of pesticides from aqueous solution.* Arabian Journal of Chemistry, 2014. **7**(1): p. 101-108.
35. Li, S., et al., *Preparation and characterization of super activated carbon produced from gulfweed by KOH activation.* Microporous and Mesoporous Materials, 2017. **243**: p. 291-300.
36. Foo, K.Y. and B.H. Hameed, *Preparation, characterization and evaluation of adsorptive properties of orange peel based activated carbon via microwave induced K2CO3 activation.* Bioresour Technol, 2012. **104**: p. 679-86.
37. Foo, K.Y. and B.H. Hameed, *Microwave-assisted preparation and adsorption performance of activated carbon from biodiesel industry solid reside: influence of operational parameters.* Bioresour Technol, 2012. **103**(1): p. 398-404.
38. Schwarz, J.S.N.a.J.A., *Estimation of the Point of Zero Charge of Simple Oxides by Mass Titration.* Journal of Colloid and Interface Science, 1988. **130**.
39. González, J.F., et al., *Pyrolysis of various biomass residues and char utilization for the production of activated carbons.* Journal of Analytical and Applied Pyrolysis, 2009. **85**(1-2): p. 134-141.
40. Dhyani, V. and T. Bhaskar, *A comprehensive review on the pyrolysis of lignocellulosic biomass.* Renewable Energy, 2018. **129**: p. 695-716.
41. García, G.B., et al., *Characterization and modeling of pyrolysis of the two-phase olive mill solid waste.* Fuel Processing Technology, 2014. **126**: p. 104-111.

42. Ersoy-Meriçboyu, D.Ö.a.A.s., *Adsorption of Copper(II) Ions onto Hazelnut Shell and Apricot Stone Activated Carbons.* Adsorption Science & Technology, 2010. **28**.
43. D. Savova, E.A., E. Ekinci, F. Yardim, N. Petrov, T. Budinova, M. Razvigorova, V. Minkova, *Biomass conversion to carbon adsorbents and gas.* Biomass and Bioenergy, 2001. **21**: p. 133-142.
44. Jun'ichi Hayashi, A.K., Katsuhiko Muroyama, A.Paul Watkinson, *Preparation of activated carbon from lignin by chemical activation.* Carbon, 2000. **38**: p. 1873-1878.
45. Okman, I., et al., *Activated Carbons From Grape Seeds By Chemical Activation With Potassium Carbonate And Potassium Hydroxide.* Applied Surface Science, 2014. **293**: p. 138-142.
46. El-Hendawy, A.-N.A., et al., *Effects of activation schemes on porous, surface and thermal properties of activated carbons prepared from cotton stalks.* Journal of Analytical and Applied Pyrolysis, 2008. **82**(2): p. 272-278.
47. Laksaci, H., et al., *Valorization of coffee grounds into activated carbon using physic—chemical activation by KOH/CO 2.* Journal of Environmental Chemical Engineering, 2017. **5**(5): p. 5061-5066.
48. Stephe Brunauer, L.S.D., W. Edwards Deming and Edward Teller, *On a Theory of the van der Waals Adsorption of Gases.* 1940. **62**.
49. Sevilla, M. and R. Mokaya, *Energy storage applications of activated carbons: supercapacitors and hydrogen storage.* Energy Environ. Sci., 2014. **7**(4): p. 1250-1280.
50. Williams, P.T. and A.R. Reed, *Pre-formed activated carbon matting derived from the pyrolysis of biomass natural fibre textile waste.* Journal of Analytical and Applied Pyrolysis, 2003. **70**(2): p. 563-577.
51. Miao, L., et al., *Design of carbon materials with ultramicro-, supermicro- and mesopores using solvent- and self-template strategy for supercapacitors.* Microporous and Mesoporous Materials, 2017. **253**: p. 1-9.
52. Wang, K., et al., *Promising biomass-based activated carbons derived from willow catkins for high performance supercapacitors.* Electrochimica Acta, 2015. **166**: p. 1-11.
53. Chang, J., et al., *Activated porous carbon prepared from paulownia flower for high performance supercapacitor electrodes.* Electrochimica Acta, 2015. **157**: p. 290-298.
54. Wang, D., et al., *High performance electrode materials for electric double-layer capacitors based on biomass-derived activated carbons.* Electrochimica Acta, 2015. **173**: p. 377-384.
55. Liu, D., et al., *A green technology for the preparation of high capacitance rice husk-based activated carbon.* Journal of Cleaner Production, 2016. **112**: p. 1190-1198.
56. Ramesh, T., et al., *Hierarchical Porous Carbon Microfibers Derived from Tamarind Seed Coat for High-Energy Supercapacitor Application.* ACS Omega, 2018. **3**(10): p. 12832-12840.
57. Rodriguez-Reinoso, F., *THE ROLE OF CARBON MATERIALS IN HETEROGENEOUS CATALYSIS.* Carbon, 1998. **36**: p. 159-175.
58. V.H, A.C.R.N.E.D.G., *Obtención de Carbón Activado a partir de Residuos Lignocelulósicos de Canelo, Laurel y Eucalipto.* Revista Politécnica, 2015. **36**(3).
59. Özçimen, D. and A. Ersoy-Meriçboyu, *Characterization of biochar and bio-oil samples obtained from carbonization of various biomass materials.* Renewable Energy, 2010. **35**(6): p. 1319-1324.
60. Román, S., et al., *Production of low-cost adsorbents with tunable surface chemistry by conjunction of hydrothermal carbonization and activation processes.* Microporous and Mesoporous Materials, 2013. **165**: p. 127-133.
61. Chen, C., et al., *Preparation and Characterization of Activated Carbon from Eucalyptus Sawdust I. Activated by NaOH.* Journal of Inorganic and Organometallic Polymers and Materials, 2013. **23**(5): p. 1201-1209.

62. Santos, J.I., et al., *Evaluating Lignin-Rich Residues from Biochemical Ethanol Production of Wheat Straw and Olive Tree Pruning by FTIR and 2D-NMR.* International Journal of Polymer Science, 2015. **2015**: p. 1-11.
63. Popescu, M.-C., et al., *Structural modifications of Tilia cordata wood during heat treatment investigated by FT-IR and 2D IR correlation spectroscopy.* Journal of Molecular Structure, 2013. **1033**: p. 176-186.
64. Yorgun, S. and D. Yıldız, *Slow pyrolysis of paulownia wood: Effects of pyrolysis parameters on product yields and bio-oil characterization.* Journal of Analytical and Applied Pyrolysis, 2015. **114**: p. 68-78.
65. Anaguano, F.A.A.V.A.H., *Determination of the point of zero charge and isoelectric point of two agricultural wastes and their application in the removal of colorants.* Revista de Investigación Agraria y Ambiental, 2013. **4**(2).
66. Dimas Suárez, J.A.M., Enrique Fuente and Miguel A. Montes-Morán, *Contribution of Pyrone-Type Structures to Carbon Basicity: An ab Initio Study.* Langmuir, 1999. **15**: p. 3897-3904.
67. J. Angel Menéndez, J.P., Bo Xia, and Ljubisa R. Radovic, *On the Modification and Characterization of Chemical Surface Properties of Activated Carbon: In the Search of Carbons with Stable Basic Properties.* Langmuir, 1996. **12**: p. 4404-4410.
68. S. K. Verma and P. L. Walker, J., *CARBON MOLECULAR SIEVES WITH STABLE HYDROPHOBIC SURFACES.* Carbon, 1992. **30**(6).
69. C. Moreno-Castilla, J.R.-U., J. P. Joly, M. V. Lopez-Ramón, M. A. Ferro-Garcia and F. Carrasco-Marín, *THERMAL REGENERATION OF AN ACTIVATED CARBON EXHAUSTED WITH DIFFERENT SUBSTITUTED PHENOLS.* Carbon, 1995. **33**: p. 1417-1423.
70. Kilic, M., E. Apaydin-Varol, and A.E. Putun, *Adsorptive removal of phenol from aqueous solutions on activated carbon prepared from tobacco residues: equilibrium, kinetics and thermodynamics.* J Hazard Mater, 2011. **189**(1-2): p. 397-403.
71. Dahlan, I., et al., *Selection of metal oxides in the preparation of rice husk ash (RHA)/CaO sorbent for simultaneous SO2 and NO removal.* J Hazard Mater, 2009. **166**(2-3): p. 1556-9.
72. SalinasTorres, D., *Tailoring of carbon materials for their use as electrodes in electrochemical capacitors* 2014, Universidad de Alicante.
73. Longart, L., *Variacion de las características morfológicas de las fibras en la madera de Pinus caribaea Var. hondurensis* U.N.E.D. GUAYANA, Editor. 2011.
74. Ould-Idriss, A., et al., *Preparation of activated carbons from olive-tree wood revisited. II. Physical activation with air.* Fuel Processing Technology, 2011. **92**(2): p. 266-270.

Figures

Figr-1

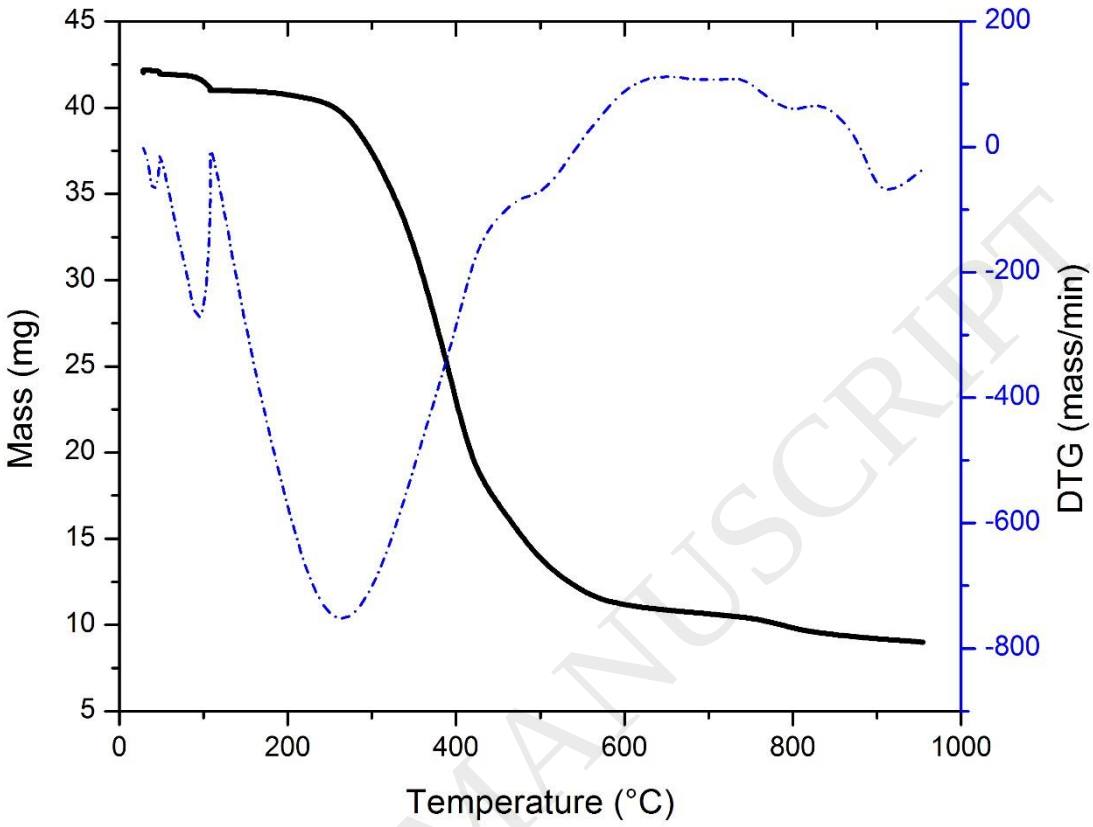

Figr-2a

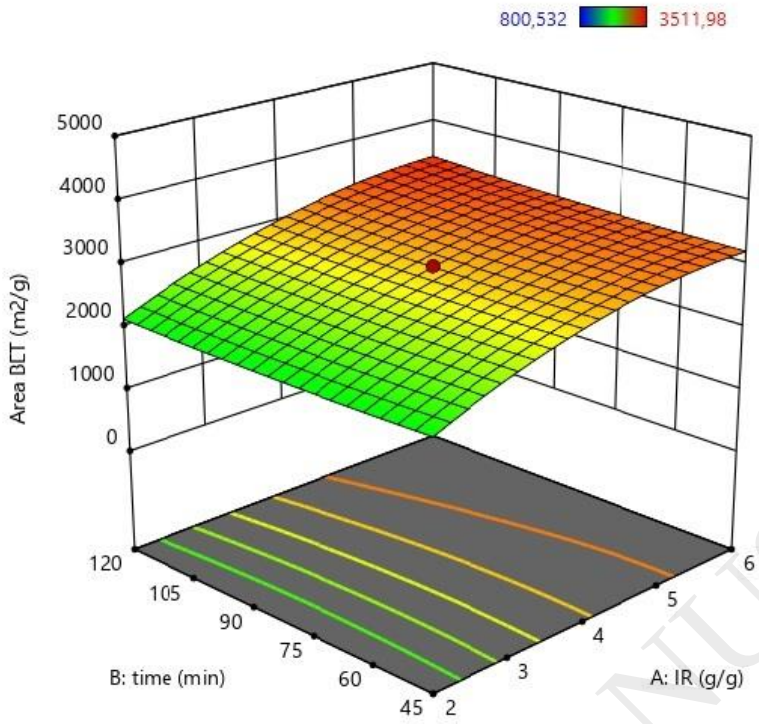

Figr-2b

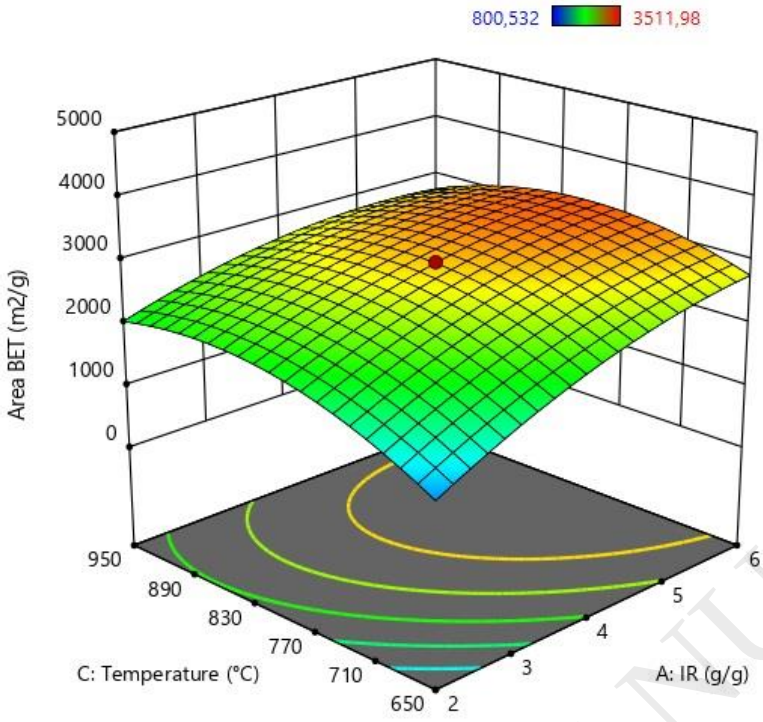

Figr-2c

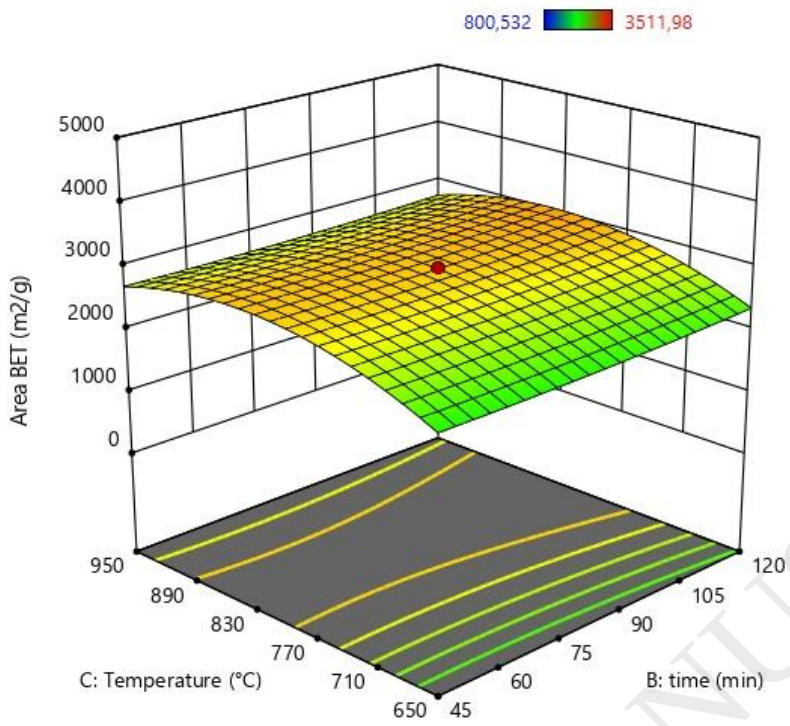

Figr-3

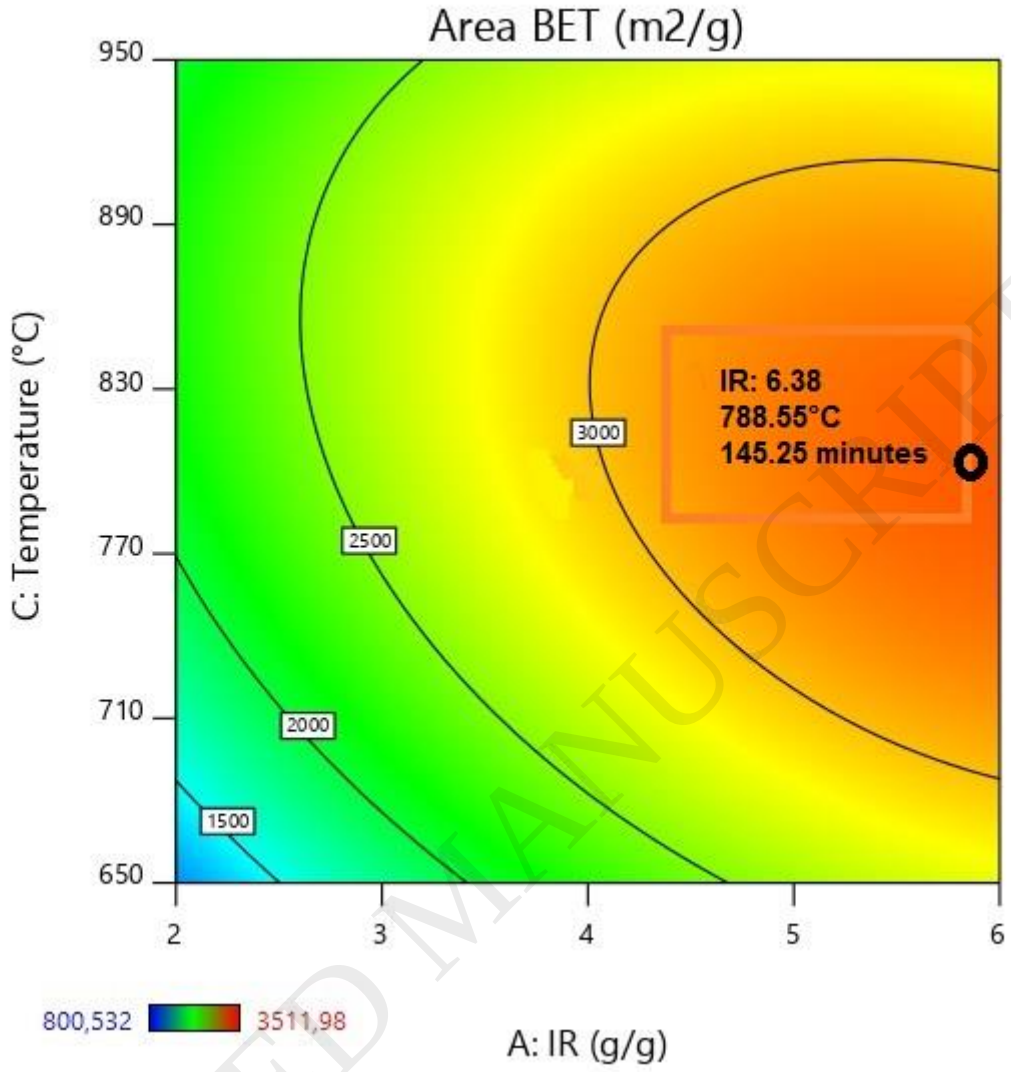

Figr-4

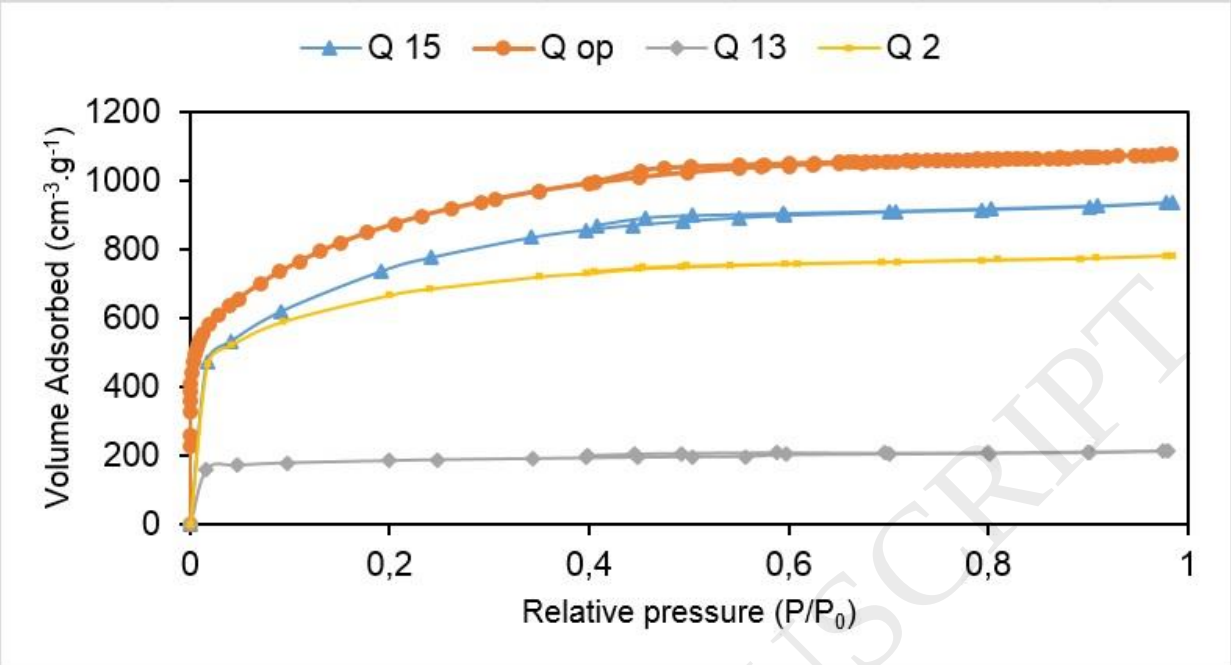

Figr-5

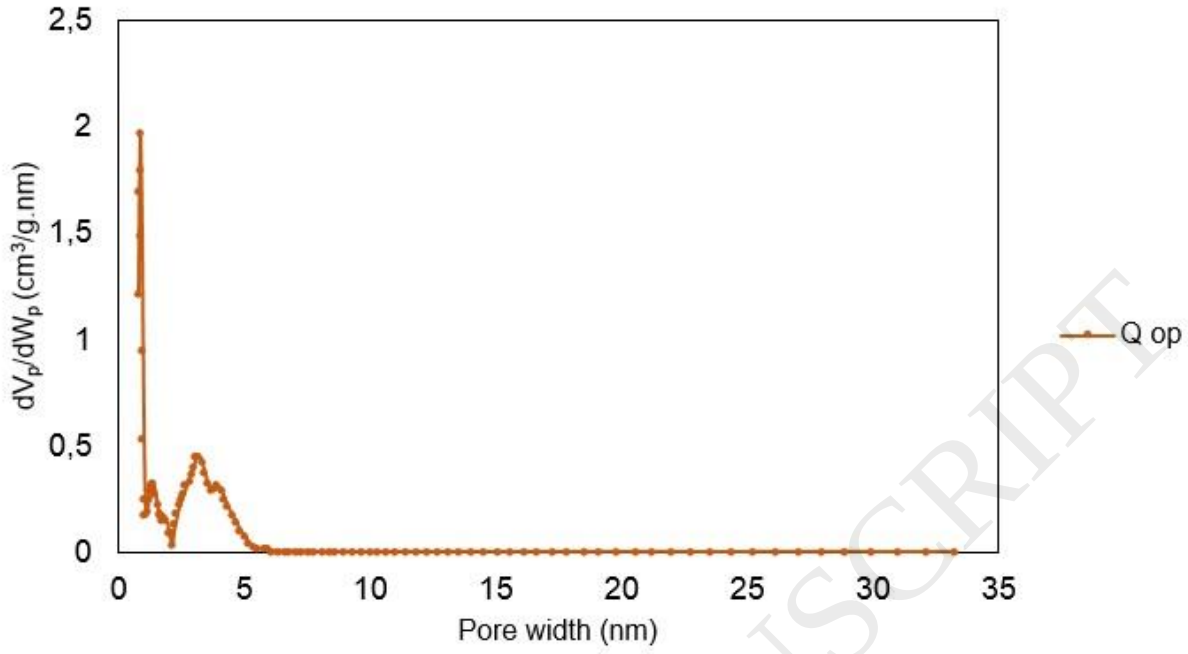

Figr-6

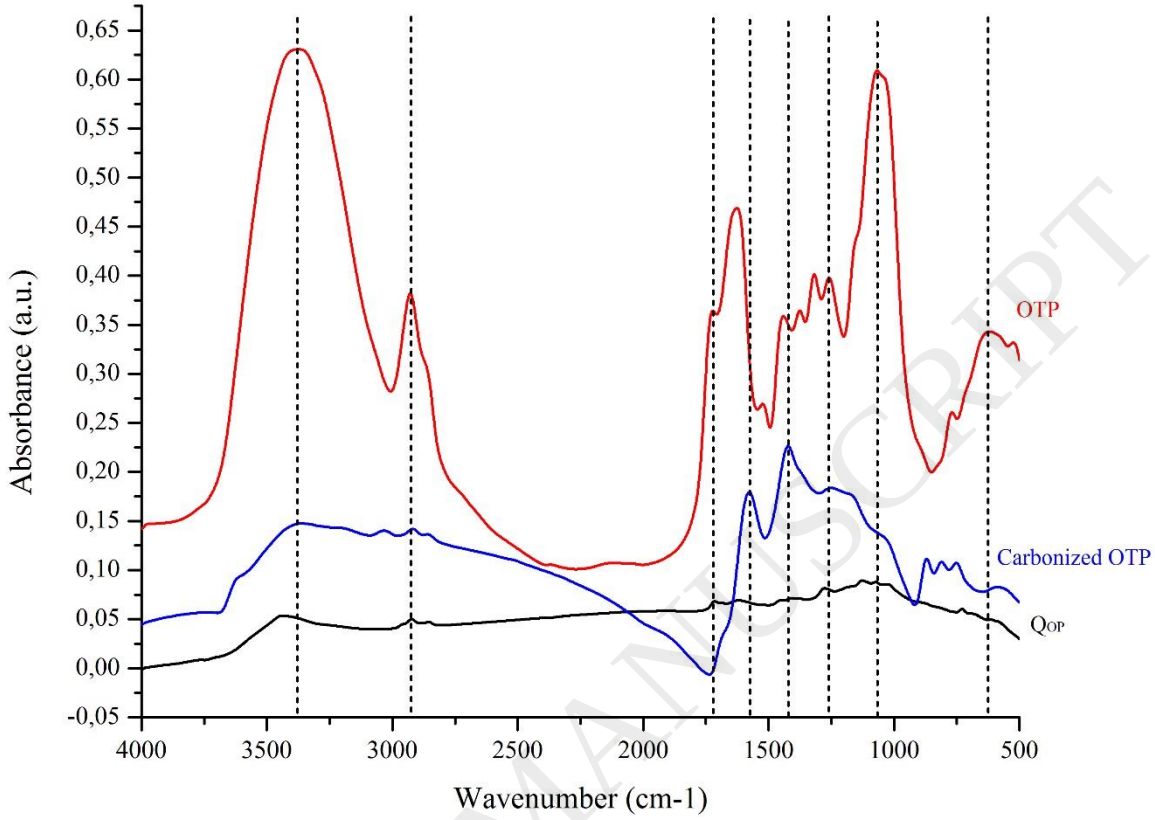

Figr-7

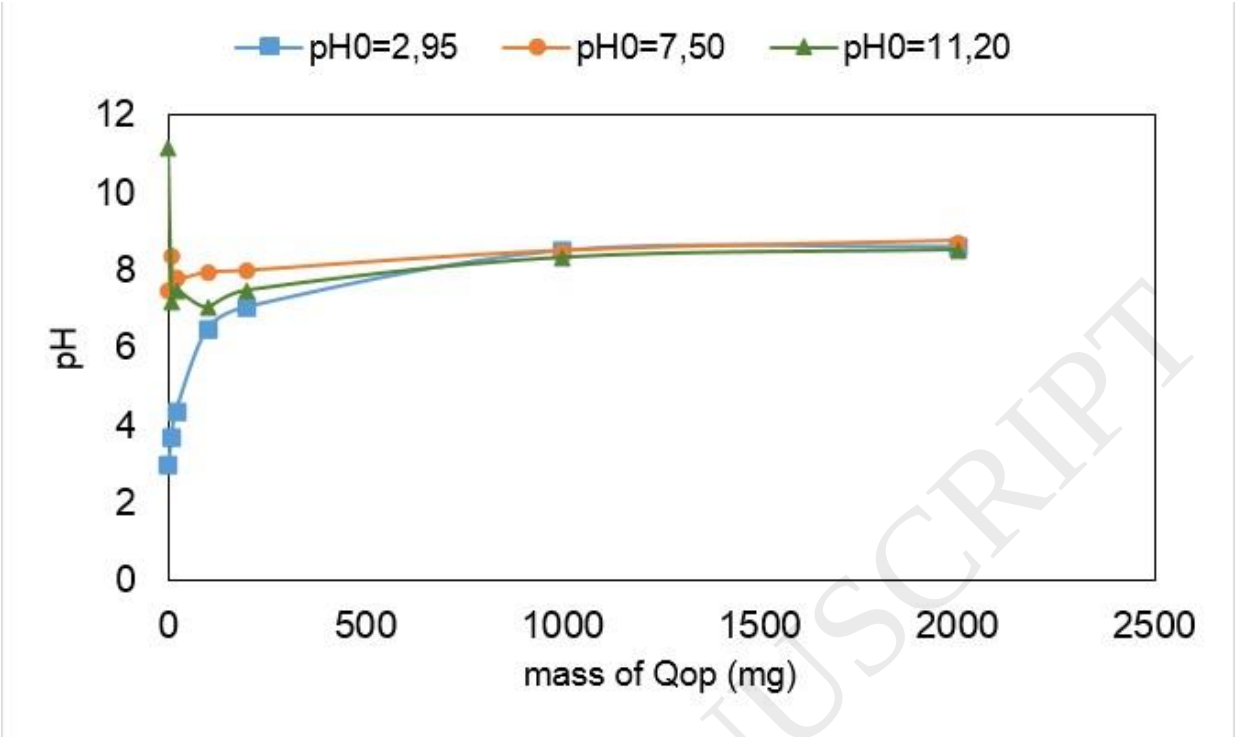

Figr-8a

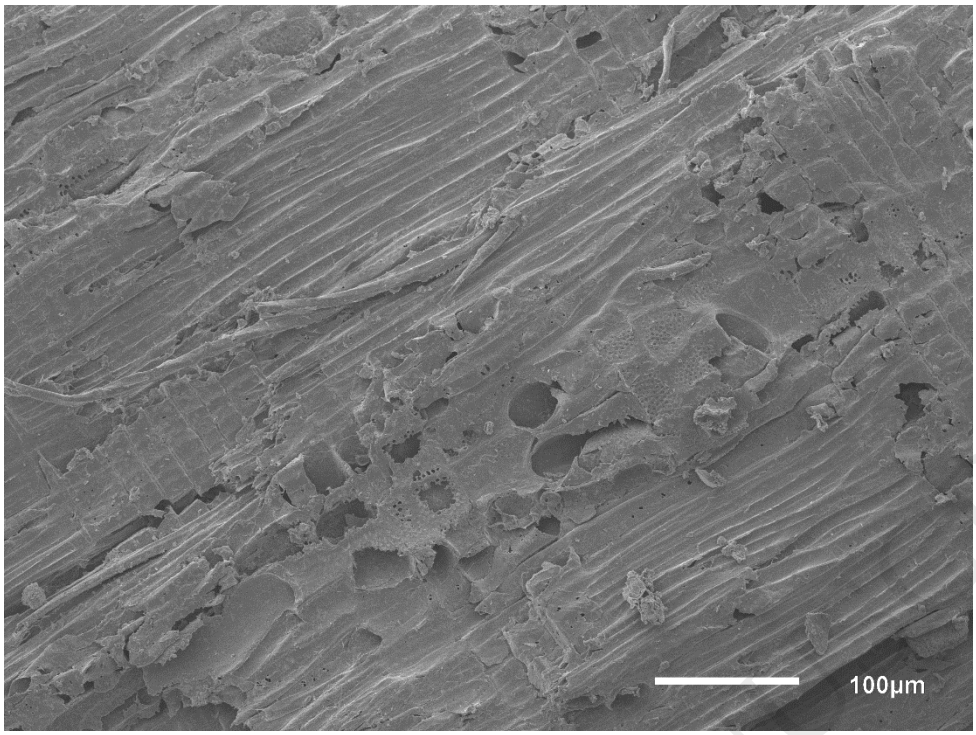

Figr-8b

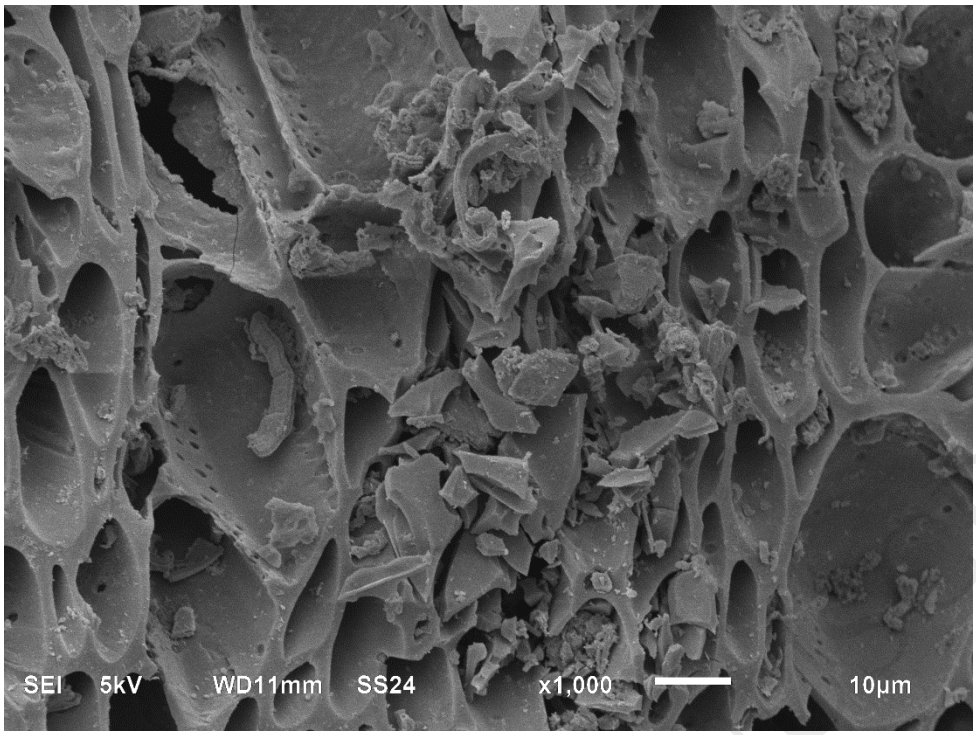

Figr-8c

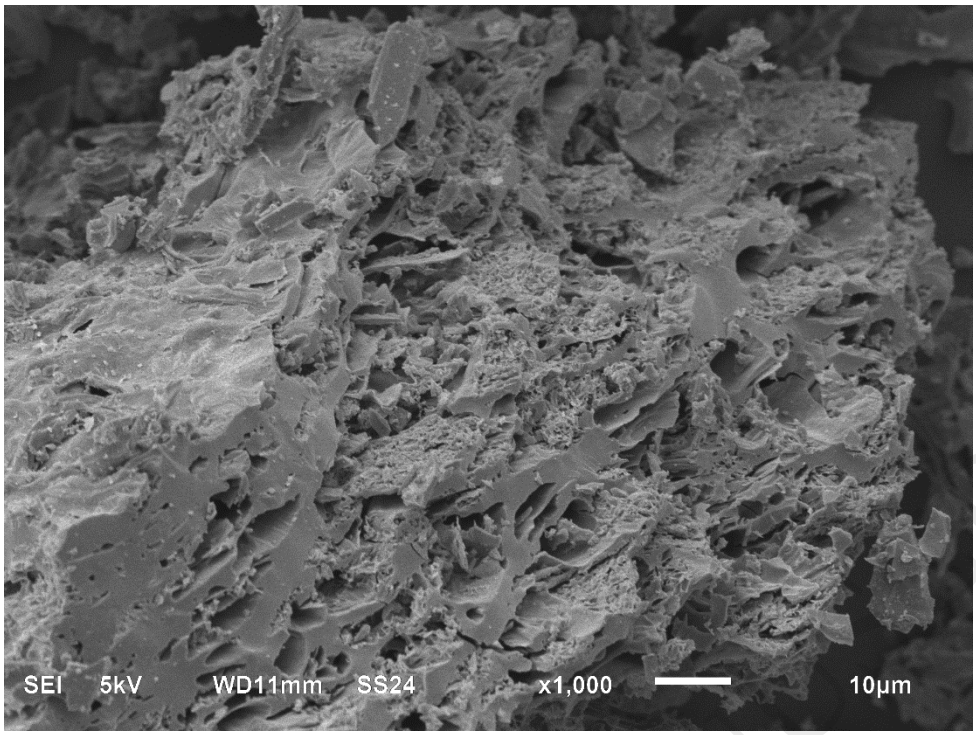

Figr-8d

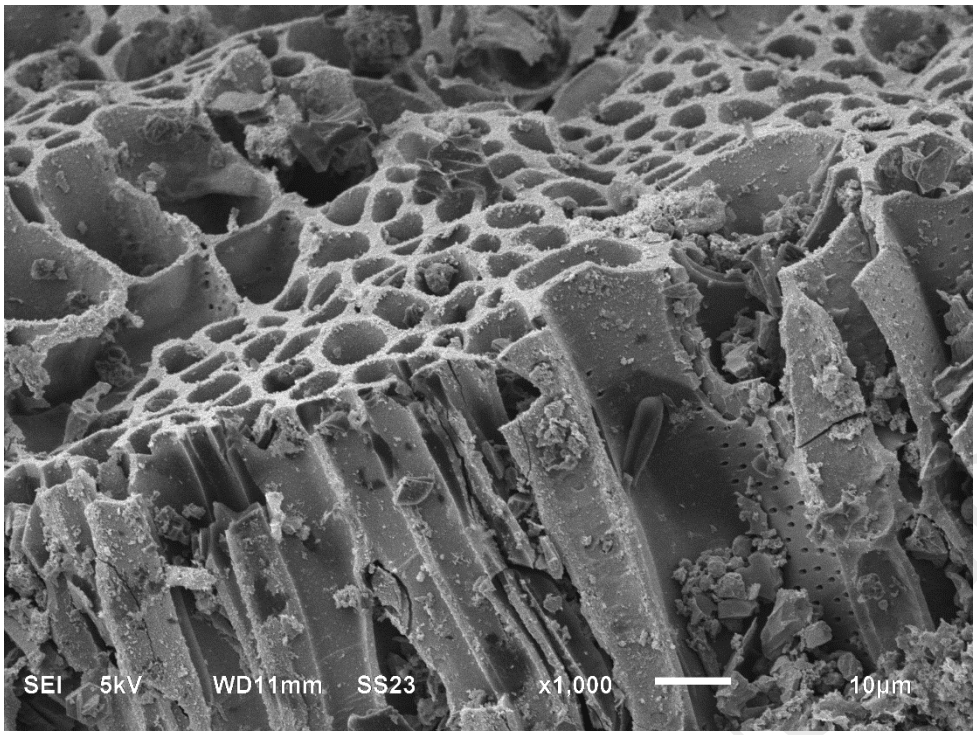

Figr-8e

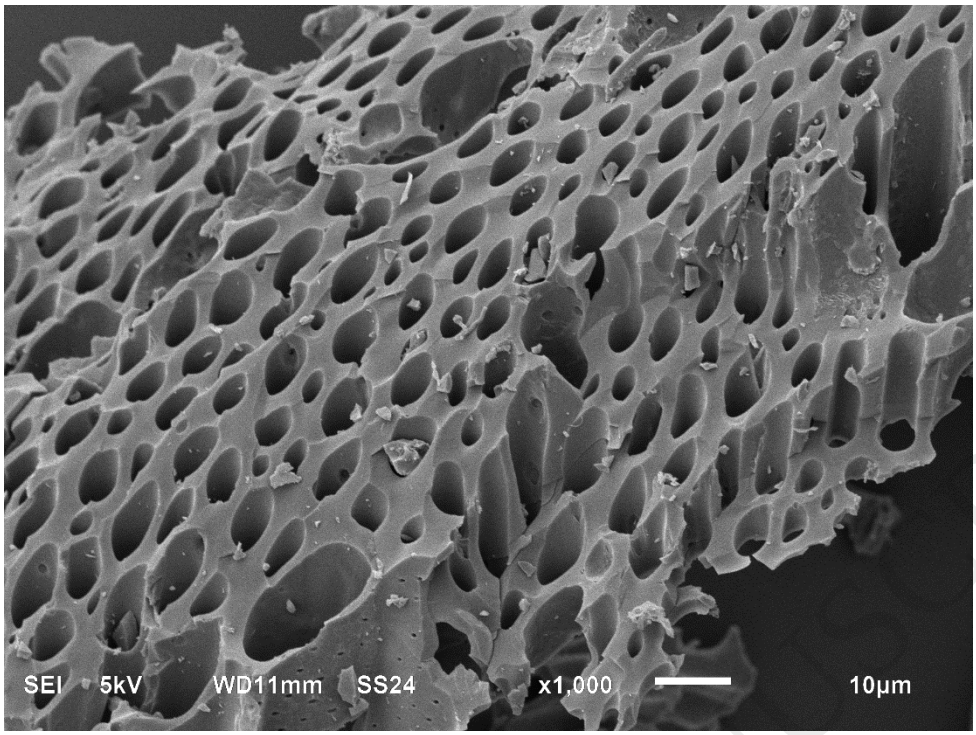

Factor	High level (+)	Low level (-)
KOH/ charcoal (A)	6	2
Activation time (B)	120 minutes	45 minutes
Activation temperature (C)	950°C	650°C

Table 1. Levels of central composite design

ID Run	A IR ($g.g^{-1}$)	B Time (min)	C Temperature (°C)
Q_1	2.00	120.00	950
Q_2	4.00	82.50	800
Q_3	2.00	45.00	650
Q_4	6.00	45.00	950
Q_5	6.00	120.00	650
Q_6	6.00	45.00	650
Q_7	2.00	45.00	950
Q_8	4.00	82.50	800
Q_9	6.00	120.00	950
Q_{10}	2.00	120.00	650
Q_{11}	4.00	19.75	800
Q_{12}	4.00	82.50	1051
Q_{13}	0.65	82.50	800
Q_{14}	4.00	82.50	800
Q_{15}	7.35	82.50	800
Q_{16}	4.00	145.25	800
Q_{17}	4.00	82.50	549

Table 2. Experimental design matrix

	Proximate (wt. %)				Ultimate (wt. %)				
	Moisture	Volatile matter	Ash	Fixed carbon	C	H	O	N	S
OTP	6.65	77.05	3.29	13.01	48.52	6.95	42.39	0.24	1.9

Lignocellulosic composition (wt. %)		
Cellulose	Hemicellulose	Lignin
47.16	25.46	15.37

Table 3. Composition of OTP

ID	Area BET(m^2/g)	Pore volume (cm^3/g)	Micropore volume (cm^3/g)	Mesopore volume (cm^3/g)	Percentage of micropore volume	Yield of activated carbon (%)
Q_1	2454.44	1.01	0.83	0.08	82.18	21.41
Q_2	2965.71	1.25	1.06	0.12	84.80	19.55
Q_3	1161.27	0.55	0.50	0.05	90.91	24.03
Q_4	2662.15	1.18	0.87	0.04	73.73	20.37
Q_5	2693.91	1.06	0.84	0.03	79.25	16.11
Q_6	2360.41	0.94	0.79	0.05	84.04	20.27
Q_7	2360.41	0.94	0.8	0.08	85.11	21.07
Q_8	2988.00	1.26	0.99	0.14	78.60	20.44
Q_9	2939.45	1.28	0.91	0.08	71.09	10.67
Q_{10}	1321.72	0.59	0.52	0.02	88.14	23.50
Q_{11}	3135.77	1.50	1.01	0.08	67.33	18.04
Q_{12}	1554.75	0.64	0.53	0.08	82.81	17.22

Q_{13}	800.53	0.33	0.27	0.06	81.82	23.26
Q_{14}	2971.65	1.60	1.09	0.03	68.13	15.86
Q_{15}	3490.00	1.66	1.09	0.04	65.66	14.00
Q_{16}	2970.24	1.61	1.08	0.03	67.08	18.82
Q_{17}	1533.63	0.63	0.54	0.06	85.17	23.13

Table 4. Experimental results of the CCD design

Source	Sum of Squares	df	Mean Square	F-value	p-value	
Block	5642.81	2	2821.40			
Model	9.256E+06	9	1.028E+06	6.95	**0.0147**	significant
A-IR	4.583E+06	1	4.583E+06	27.54	**0.0019**	significant
B-time	25448.65	1	25448.65	0.1529	0.7093	
C-Temperature	6.246E+05	1	6.246E+05	3.75	0.1008	
AB	15870.77	1	15870.77	0.0954	0.7679	
AC	3.981E+05	1	3.981E+05	2.39	0.1729	
A^2	8.866E+05	1	8.866E+05	5.33	0.0604	
B^2	16063.00	1	16063.00	0.0965	0.7666	
C^2	2.792E+06	1	2.792E+06	16.77	**0.0064**	significant
Residual	9.968E+05	5	1.664E+05			
Cor Total	1.026E+07	16				

Note: R2=90.26% R2 adjusted=77%

Table 5. ANOVA of OTP activated with KOH

Precursor	Conditions	Surface Area ($m^2.g^{-1}$)	Reference
Olive tree pruning	KOH/charcoal 6.38:1 788°C 145 minutes	3514	This work
Willow catkins	KOH/charcoal 1:1 800°C 60 minutes	1586	[52]
Hazelnut bagasse	KOH/charcoal 3:1 700°C 120 minutes	1642	[23]
Paulownia flower	KOH/charcoal 4:1 800°C 60 minutes	1471	[53]
Corncob	KOH/charcoal 4:1 750°C 180 minutes	2701	[54]
Rice Husk	KOH/charcoal 4:1 700°C 60 minutes	3263	[55]
Tamarind seed coat	KOH/charcoal 3:1 800°C 60 minutes	1702	[56]
Jatropha wood	KOH/charcoal 1:1 70°C 120 minutes	1305	[12]

Table 6 Conditions and surface area values (m^2/g) for activated carbons with KOH obtained from different precursors

OTP (cm^{-1})	Carbonized OTP (cm^{-1})	Q_{OP} (cm^{-1})	Functional groups	Class of compounds	Reference
3378	3380	3443	O-H stretching	Polymeric O-H, water impurities	[58]
2928	2915	2922	C-H stretching	Alkanes	[42]
1720	-	-	Stretching C=O	Carbonyl groups	[59]
1626	1578	1624	C=O asymmetric stretching	Carboxylic groups	[35]
1522	1514	-	C=C stretching of aromatic skeletal	Alkenes	[60]
1427	1428	-	C-H deformation	Carboxyl groups	[61]
1258	1251	1279	C-O-C stretching	Ester	[62]
1058	-	-	C-O stretching vibrations	Cellulose and hemicellulose	[63]
769	750	728	O-H bending	Aromatic compounds	[64]

Table 8 Assignment of FTIR bands to OTP, carbonized OTP and Q_{op} surface functional groups